

Step-by-step observation of the hydration of C_3S by magic-angle spinning ^{29}Si nuclear magnetic resonance: the masking effect of D_2O

A. COMOTTI, G. CASTALDI, C. GILIOLI

Italcementi S.p.a., Central Research and Development Department, via G. Camozzi, 124 Bergamo 24100, Italy

G. TORRI

Istituto Ronzoni, via G. Colombo, 81 Milano 20133, Italy

P. SOZZANI*

Dipartimento di Ingegneria Meccanica, Università di Brescia, via Branze, 38 Brescia 25123, Italy

High-resolution solid-state ^{29}Si nuclear magnetic resonance (NMR) characterization of hydrated C_3S provides a means of selectively observing the hydrogen-containing phases. In particular, by applying the cross-polarization (CP) technique, we demonstrated that a contrast can be obtained, not only for hydrated against anhydrous phases, but also for hydrogen-hydrated against deuterium-hydrated phases. Selectively deuterated samples were thus prepared by a H_2O/D_2O alternated hydration procedure. The progress of the polycondensation of orthosilicates as derived by H_2O was followed, demonstrating that a separate microphase of anhydrous C_3S prevalingly reacted at any step. An induction period, showing a low reactivity and mainly formation of Q^0 hydrated was observed during the first hydration steps of selectively deuterated samples. The efficiency of the masking effect of D_2O was also indirectly proven by comparison with calorimetric measurements.

1. Introduction

During the last few years it has been demonstrated that magic angle spinning (MAS) nuclear magnetic resonance (NMR) is a valuable method for obtaining a wider knowledge of the structure of cement-based materials. The main advantage of this technique over the traditional methods is the possibility of following the evolution of species in the amorphous phase.

In particular, the degree of condensation of SiO_4^{4-} tetrahedra were singly detected by measuring the content and the length of the orthosilicate polymers [1]. At the same time, the crystalline structure of anhydrous C_3S can be identified from its multiplicity of sharp signals, each of which is associated with a different crystalline environment [2].

On this basis, several phenomena were addressed by this technique, including the effect of silica fume, $CaCl_2$ and sucrose on the evolution of the reacting species [3, 4]. The result of the carbonation process was also identified by the increased formation of branched SiO_4^{4-} structures [5].

Published papers have identified the distribution of the species at a certain time as the cumulative product

of the reactions from the beginning of the hydration process. In the present work we suggest the use of D_2O as an agent to mask the initial steps of hydration. This was made possible by using H_2O only in the second step of the process. As a matter of fact, a procedure was developed by which two different phases were obtained (both were hydrated, one by deuterium, the other by hydrogen). ^{29}Si atoms belonging to the phase containing hydrogen can be selectively detected by exploiting the phenomenon of $^1H-^{29}Si$ cross polarization [6].

2. Experimental procedure

2.1. Preparation of the samples

The synthesis of C_3S was carried out using stoichiometric quantities of calcium carbonate and silica. The mixture was heated several times at $1450^\circ C$, after repeated grinding, until equilibrium conditions were reached. The product was characterized, as-obtained, by X-ray diffraction (XRD), by optical microscopy and by ^{29}Si solid-state NMR. It was identified as triclinic C_3S containing a small amount of CaO

* Author to whom correspondence should be addressed.

(< 0.5%). The C_3S powder, typically 400 mg, was hydrated for 1.5, 3, 4.5, 6 and 9 h with D_2O (with a water-to-solid ratio of 0.5) under an N_2 atmosphere at 20 and 30 °C, as described in Section 3. The hydration process was quenched by the addition of an excess of acetone, and the sample was dried under a vacuum. Alternatively, the sample was freeze-dried without an addition of acetone. In a second step, the hydration was started again by treatment with H_2O for a time ranging from 1.5 to 3 h. The drying process was carried out as described above. This procedure was also applied using H_2O in the first step and D_2O in the second step.

2.2. X-ray diffraction

XRD profiles of the powders were obtained with a Siemens D5000 Diffractometer, using CuK_{α} radiation and a diffracted-beam monochromator.

2.3. Calorimetry

Isothermal calorimetry was carried out by using a home-made instrument developed by Costa [7]. The experiment follows the Cembureau recommended procedure for the measurement of the heat of hydration of cement by the conduction method.

2.4. NMR

High resolution ^{29}Si MAS NMR spectra were run at 59.6 MHz on a CXP300 Bruker instrument operating at a static field of 7.4 T. An MAS Bruker probe was used with 7 mm ZrO_2 rotors spinning at a standard speed of 5 kHz. Cross-polarization spectra were collected with contact times of 2 ms and the proton decoupling power was set at 800 W. Relaxation measurements of ^{29}Si T_1 were performed by the Torchia method [8]. Care was taken to acquire the same number of scans (12 000 transients) and to set all the experimental parameters to the same values. MAS experiments without cross polarization were run with recycle times of 300 s and a pulse length on ^{29}Si of 4 μs . 1H decoupling power was turned off. Quantitative MAS experiments were performed by applying a delay time of 500 s. A Q_8M_8 sample (trimethylsilylester of octameric silicic acid, $Si_8O_{20}H_8$) was used as the second standard, assigning the ^{29}Si chemical shift of the trimethylsilyl groups to + 11.5 ppm (parts per million) from Me_4Si [9]. The Q_8M_8 area response was retained as a reference for the total-spectral-area estimation.

3. Results and discussion

Tricalcium silicate (C_3S) is the main reactive component of Portland cement and most chemical processes in the early stages of hydration take place in this phase [10]. Therefore, pure C_3S was synthesized, characterized, and later subjected to the reaction with water.

C_3S , after conditioning at 1450 °C, was ground and sieved in order to obtain particles less than 90 μm in

size. The progress of the hydration was followed for a short time, during which less than 5% of the reaction took place. The anhydrous phase is known to remain in the system after a prolonged hydration time, at the usual H_2O/C_3S ratio of 0.5, being shielded by the outer hydrated part of the particles during the diffusion of water.

Thus, the following discussion was aimed at the study of both the anhydrous C_3S and the hydrated phases.

3.1. Characterization of C_3S

The ^{29}Si MAS NMR spectrum of C_3S , as-obtained, is presented in Fig. 1. Eight sharp peaks appeared in the range - 69.05 to - 74.68 p.p.m. from TMS.

The chemical shift, CS, the line width, LW, and the peak area, PA, as obtained by the deconvolution treatment, are reported in Table I. The high resolution allowed the CS measure to be for each peak with a

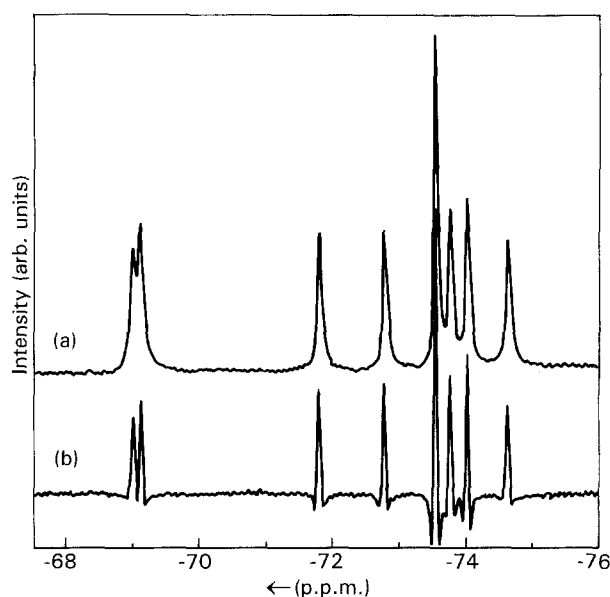


Figure 1 ^{29}Si MAS NMR 59.6 MHz spectrum of C_3S , with a recycle time of 300 s: (a) no resolution enhancement was applied; (b) the spectrum obtained with a Lorentzian resolution enhancement (Line Broadening = - 6, Gaussian Broadening = 0.7).

TABLE I Chemical shifts (CS), line widths, (LW), and the peak area (PA) for anhydrous tricalcium silicate

Signal Number	Chemical shifts from TMS p.p.m.	Line width (Hz)	Peak areas ^{a,b}	Idealized areas
1	- 69.05	6.2	0.99	1
2	- 69.17	5.6	1.02	1
3	- 71.85	5.4	1.01	1
4	- 72.82	5.4	1.01	1
5	- 73.59	4.4	1.99	2
6	- 73.81	5.1	0.99	1
7	- 74.06	4.3	0.96	1
8	- 74.68	5.8	1.03	1

^a The Peak areas were normalized for obtaining a total area of 9 and, after dividing the peak number 5 by a factor of 2, an arithmetic mean a_{AV} of 1. The standard deviation, estimated from $\sigma = [\sum_i (a_i - a_{AV})^2 / (n - 1)]^{1/2}$, is equal to 0.02.

considerable precision and (only for the two downfield signals, at -69.05 and -69.17 p.p.m.), partial overlapping occurred. The CS values were estimated from the deconvolution process.

The spin-lattice relaxation parameters were not measured, because of the very long time required when being estimated T_1 values are longer than hundreds of seconds. However, the recycle time was made sufficiently large (300 s) to obtain the balance of the signal response, as can be demonstrated by observation of the peak areas in Table I. The signals were close to the idealized ratios of 1 or 2, within a 5% approximation. The standard deviation equalled 0.02, indicating a narrow distribution (see Table I).

The CS seems to be linearly correlated to the Si–O average distance of the SiO_4^{4-} tetrahedra in the triclinic C_3S cell [11]. This has been already suggested by comparison with the spectra of other silicates [12]; nevertheless, the assignments are not in agreement with those given in recent works, taking into account a more specific set of data [13]. Given the high resolution obtained in the present work, the difference in the CSs of the closest peaks (0.12 p.p.m.) should correspond, in the interpretations of [11, 12] to a difference in the distances of a very small fraction of an Angstrom. A revision of the peak assignments, and of the general interpretation, is in progress [14].

Even at the degree of resolution that we obtained, and applying resolution functions before Fourier transformation (Fig. 1b), signal number 5 was not split. Signal number 5 was one of the narrowest signals (LW = 4.4 Hz). This fact indicates a substantial equivalence of two silicon environments, although the unit cell determined by XRD is described by nine different silicon atoms.

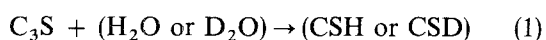
As an indication of the purity of the C_3S sample, no signal due to C_2S at -71.34 p.p.m. was detected. A small percentage of any impurity should have been recognized, because no overlapping occurs in this region. The mixture of the two compounds has been identified, for example, in [2].

On the basis of the characterization above, we can draw the conclusion that the sample under observation is fully composed of highly crystalline triclinic C_3S .

3.2. Hydration of C_3S by H_2O and D_2O

We focused on the early stages of hydration (within 10 h of hydration). The hydration process was divided in two steps: in the first step D_2O was used for varying times; in the second step H_2O was added to the dried sample and it was left to react for a given time (generally, 1.5 h). Fig. 2 gives timetable for the hydration procedure for the different samples (group 1, A–E). Group 2 contained the samples hydrated by H_2O for longer time. Samples hydrated by H_2O alone for the same total time were prepared for the sake of comparison.

The protons or the deuterons enter the reaction



thus hydrated (CSH) or deuterated (CSD) species are

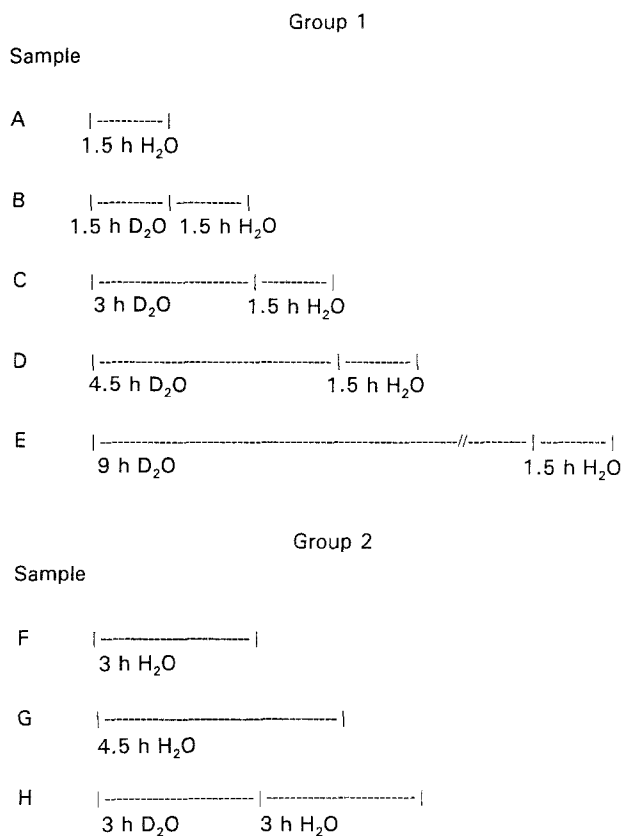


Figure 2 Samples of C_3S exposed to D_2O for various times and subsequently to H_2O for 1.5 h (group 1) and to H_2O for longer times (group 2).

formed. By this method a mixture of CSH and CSD samples can be formed. Protons or deuterons are also present in the surrounding silicate oligomers in the form of immobilized water. This water was observed by ^1H MAS NMR [14].

^1H – ^{29}Si cross-polarization pulse-sequencing selectively detects the ^{29}Si atoms placed in an environment of ^1H atoms, even if they are not covalently bonded [6]. In general terms, the cross-polarization phenomenon is dominated by spin diffusion over a range of a few nanometres. Therefore, it only reveals the silicon atoms presenting intimate relationships with hydrogen atoms belonging to the same phase. On the other hand, the MAS experiments showed the presence of both the anhydrous and the hydrated phases. Therefore, MAS NMR and CPMAS NMR experiments can discriminate between the different phases and they can be considered as complementary techniques for the understanding of the C_3S hydration process. The deuterated phase acts as a masking agent for the CP phenomenon, since it cannot be detected even if the hydration process has progressed. As a matter of fact, no ^{29}Si signal was detected when the D_2O hydrated samples were observed under cross-polarization conditions (not shown).

Samples hydrated by H_2O alone were also considered. Fig. 3 shows MAS and CPMAS NMR spectra of a sample hydrated for 1 month. The MAS spectrum was recorded with a recycle time of 500 s. The region from -69.05 to -74.68 p.p.m. (Q^0) describes the unreacted crystalline C_3S phase (Fig. 3a). The peaks at -79.0 and -84.8 p.p.m. correspond to the Q^1 and

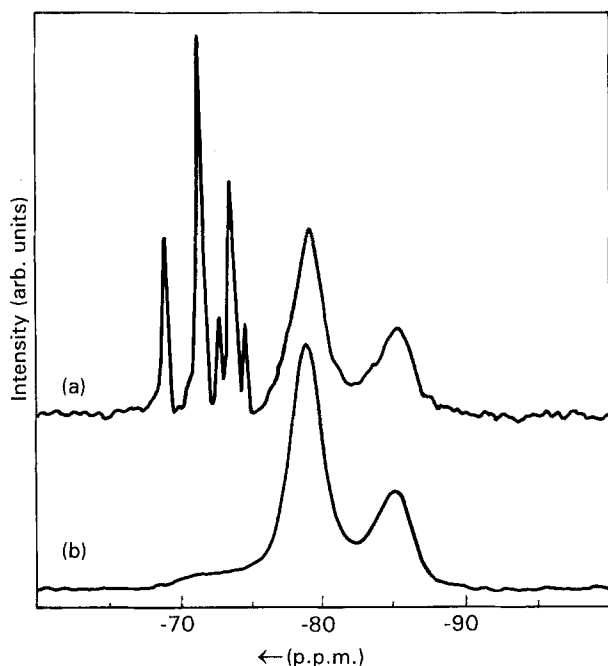


Figure 3 (a) A ^{29}Si MAS NMR 59.6 MHz spectrum of partly hydrated C_3S run with a recycle time of 500 s. The eight peaks from -69.05 to -74.68 p.p.m. from TMS correspond to the anhydrous C_3S in Fig. 2; Q^1 and Q^2 units (at -79 and -84.8 p.p.m. respectively) are assigned to the polymerized species. (b) A ^{29}Si CPMAS NMR 59.6 MHz spectrum of the same sample.

Q^2 species formed during the hydration process. The CPMAS experiment (Fig. 3b) exhibits only the Q^0 , Q^1 and Q^2 species in the hydrated phase. In particular, the shoulder at -73.5 p.p.m. (Q^0) is due to the SiO_4^{4-} units in the hydrated phase.

A typical ^{29}Si CPMAS spectrum of samples A–E (Fig. 2, group 1) is shown in Fig. 4. The spectra were

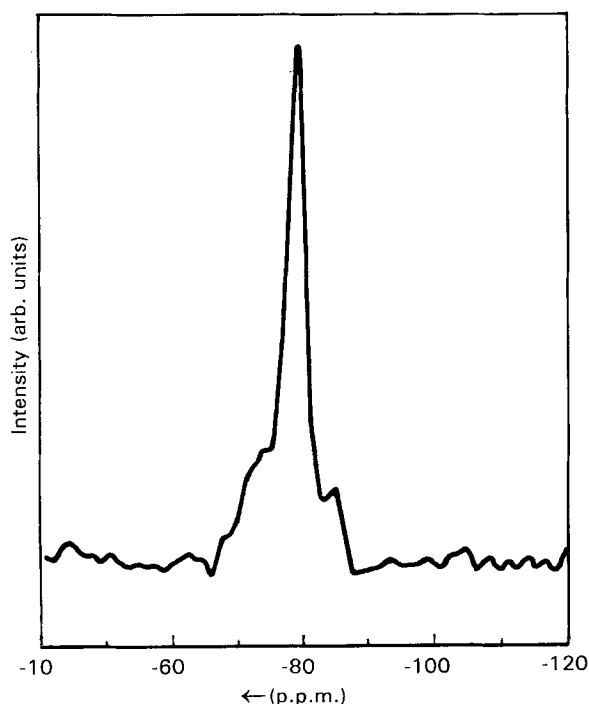


Figure 4 A ^{29}Si CPMAS 59.6 MHz spectrum of a sample hydrated for 3 h with D_2O and for 1.5 h with H_2O (see Fig. 2, group 1, C).

evaluated under two aspects:

- (i) the distribution of the polymerized species in a sample;
- (ii) the total intensity of the spectrum, measured under *strictly* the same conditions, indicating the total amount of hydration occurred.

For (i), the distribution of the species keeps the same pattern for the same time of hydration (typically 1.5 h), independently of the length of time of the prereaction with D_2O , except for sample A in which a larger amount of Q^0 is observed (see later). The time of hydration with H_2O affects the distribution, leading to an increasing Q^2 content. Taking into account that each linear polymerized species (n monomeric units) contains two chain ends (Q^1) and $n - 2$ internal monomer units (Q^2), the length of the chain (chain \geq dimer) can be expressed in terms of the ratio q^2/q^1 (where q^x denotes the percentile amount of each species Q^x) and in terms of a response factor, f . The different amounts q^0 , q^1 , q^2 measured separately, and a semiquantitative analysis can be performed in order to calculate the average length of the oligomers and the degree of polymerization. The contact times of the cross polarization may affect the relative response of the species, and suitable correction factors must be measured [3] by the formula

$$n = 2(fq^2/q^1) + 2 \quad (2)$$

The response factor is dependent on the mixing time in the cross polarization experiment. Therefore, the intensity of the signals for Q^1 and Q^2 was measured as a function of the mixing time adopted in the experiments (Fig. 5). During the mixing time, the ^{13}C magnetization grew along a typical curve with a maximum. This is due to the competition between the magnetization transfer from hydrogen (associated with the ^{29}Si – ^1H cross polarization rate T_{SiH}) and the relaxation in the rotating frame ($T_{1\rho\text{H}}$) [15]. The signal intensities at increasing mixing times were interpolated by a non-linear least-squares procedure, according to the formula

$$I = I_0 [\exp(-\tau/T_{1\rho\text{H}}) - \exp(-\tau/T_{\text{SiH}})] \times (1 - T_{\text{SiH}}/T_{1\rho\text{H}}) \quad (3)$$

where I is the magnetization, I_0 is the equilibrium magnetization and τ is the variable contact time. T_{SiH} and $T_{1\rho\text{H}}$ were thus measured (0.4 ms and 5.6 ms respectively for Q^1 species; 0.6 ms and 10.5 ms for Q^2 species). 500 s relaxed MAS spectra provided the reference composition (Fig. 3). In fact in our dried samples, relaxation times ^{29}Si T_1 of the order of more than 100 s were measured. By a comparison of the CPMAS experiments and the MAS experiments, we deduced that the response factor, f , is equal to 1 by using mixing times of 2 ms (which falls in the range of the maximum intensity of the signals).

The distribution and the average degree of polymerization are given in Table II for different hydration times. They are in agreement within 10% with the evaluation published by Rodger *et al.* [16]. Care was taken to characterize the samples for the same times after the hydration process, in order to reduce any

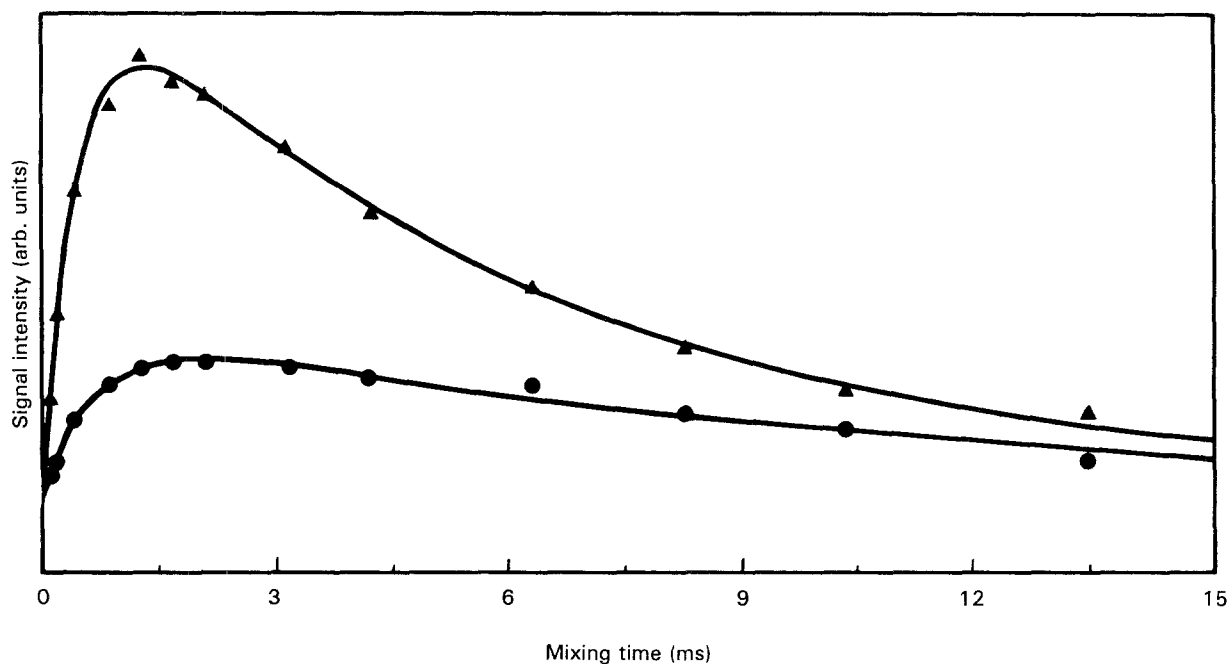


Figure 5 Interpolation of the signal intensities at increasing mixing times by a non-linear least-squares formula. (▲) signal intensity due to Q^1 species and (●) signal intensity due to Q^2 species.

TABLE II

Hydration time (H_2O)	q^0 (%)	q^1 (%)	q^2 (%)	n
1.5 h	12	82	6	2.2
1 gg	13	76	11	2.3
3 gg	10	65	25	2.7
1 month ^a	9	62	29	2.9

^a Anhydrous Q^0 is present in the same amount as Q^1 (shown by evaluation of the MAS spectrum of Fig. 3a).

possible contribution from the condensation which takes place in the dried material, that, however, is considered to be a minority under the ageing times adopted.

We believe that the condensed species distribution may act as a fingerprint of the time passed after the beginning of the hydration of that phase. The evidence that the hydrated chain length is not affected by the deuterated chain length (any time of D_2O prereaction or no D_2O prereaction at all) is in agreement with a separate phase process, and thus fresh C_3S is hydrated at each step. The ratio q^2/q^1 measured in sample A (H_2O only) is the same as in samples B–E although the amount of Q^0 is slightly larger in sample A. If mixed H/D oligomeric species were present, a higher

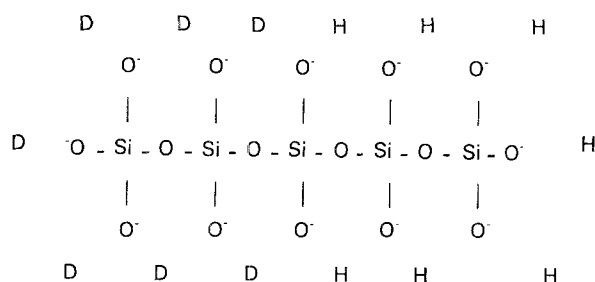


Figure 6 An example of the species formed during the hydration process.

q^2/q^1 ratio would be expected in the CP spectrum, as shown in Fig. 6.

On the other hand, in order to focus on point (ii) above, the total area of the spectra were estimated for each sample (Fig. 2, group 1, A–E). The comparative results, given an identical spectrometer response, obtained by keeping the experimental conditions strictly constant (see Section 2), were plotted as an histogram in Fig. 7. The total intensity is indicated in arbitrary units on the ordinate axis and the D_2O reaction time (hours) on the abscissa axis.

The quantity of the hydrogen-containing phase apparently depends on a complex way on the D_2O prehydration time. The trend is characterized by a minimum, about 1.5 h after the hydration by D_2O started; the hydration process is sensibly more active in the initial stage. Longer times of prehydration, after the minimum, lead to a slow recovery of the signal intensity from the minimum value.

A few internal checks of the consistency of the results were derived by a comparison of the total areas of the spectra for a time corresponding to the sum of times before measured. For example, the area for sample H (Fig. 2, group 2) equals the sum of the areas of samples C + D within a 15% error. Also, other

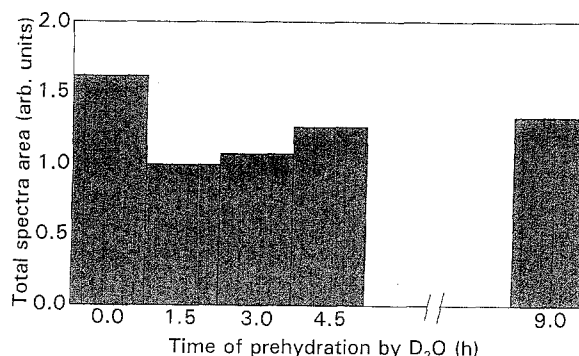


Figure 7 A total-area-values histogram for each sample in group 1 of Fig. 2.

groups of data demonstrate the correctness of the results; the only exception is that the area of sample A (1.5 h H₂O) is equal to that of sample F (3 h H₂O), although the hydration time was twice as long. Thus almost no progress of the reaction occurred between 1.5 and 3 h. The intermediate depression of the trend can be explained by the development of an intense heat followed by a *dormient* stage [10].

In the case of D₂O the isotope effect on the hydration led to a slower rate in comparison with the H₂O hydration. This is in agreement with the results due to King *et al.* [17]. On the other hand, another kind of isotope effect may be present: that is a possible H/D exchange on the preformed hydrated species. In order to check the ineffectiveness of the H/D exchange, a reverse experiment was performed, by which a H₂O-hydrated sample was exposed to D₂O for a longer time than the average of the times applied. A reduction of the NMR response should occur in the presence of H/D exchange. This fact was not observed within the experimental error.

3.3. Calorimetric results

Calorimetric experiments were performed by following the heat evolution due to the H₂O hydration on samples which had previously been subjected to a variable-time D₂O hydration, by analogy with the process of obtaining samples A–E. The heat output was developed in each case within the first minutes of the runs. The integrals followed the same trend as the NMR experiments (Fig. 7).

This confirms that C₃S is available for the hydration at every step, indicating that an effective physical barrier does not exist for the new H₂O hydration.

3.4. Induction-period observation

In order to observe carefully the depression of the signal intensity and the distribution of the species during the induction period, we applied the general procedure presented above to slower reaction rates. Therefore, a set of H₂O- and D₂O/H₂O-hydrated

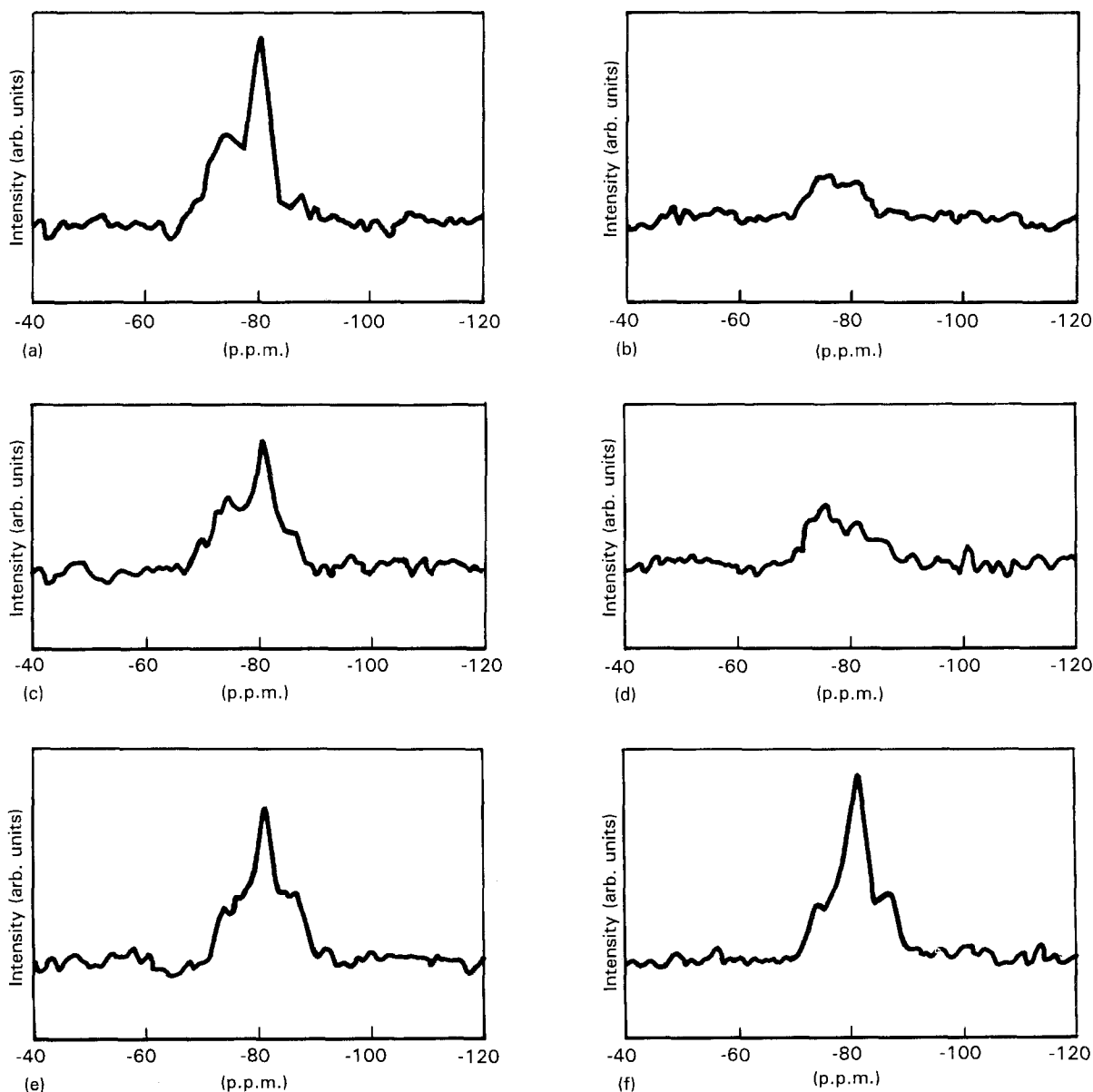


Figure 8 ²⁹Si CPMAS 59.6 MHz spectra for C₃S hydrated at 20 °C for different times by H₂O and by D₂O/H₂O: (a) 1 h H₂O; (b) 1 h D₂O, and 1 h H₂O; (c) 2 h H₂O; (d) 2 h D₂O, and 2 h H₂O; (e) 4 h H₂O; and (f) 4 h D₂O, and 4 h H₂O.

samples was prepared at a lower temperature ($T = 20^\circ\text{C}$).

It is apparent from Fig. 8 that a marked decrease of the response is obtained if the H_2O -hydration time covers the induction period (this is observed, in particular, in Fig. 8b). This demonstrates that D_2O is able to mask the preceding steps of hydration.

In particular, we observed that the amount of Q^0 is proportionally much larger during the induction period in comparison to the first hour of hydration.

By this experiment we could clearly show that the distribution of the species is different during the evolution of the reaction in the step-by-step observation of the system.

4. Conclusion

The MAS NMR characterization of hydrated C_3S not only provides selective detection of the anhydrous and amorphous phases, but also an opportunity to contrast portions of the sample as hydrated by H_2O and D_2O .

The process of isotopically labelled hydration offers, therefore, a new tool for evaluating the step-by-step hydration of C_3S . A minimum of activity was found between 1.5 and 3 h. At this stage a major amount of anhydrous C_3S is still present in the system. This supports the hypothesis of a physical reason for the initial reduction in the rate of diffusion of water [10].

On the other hand, the progress of the polymerization of orthosilicate, in the C_3S particles, was followed selectively at specific stages of hydration for the first time. No difference was observed in the chain-length distribution of the chains at the different stages, except during the induction period, indicating that short chains can be formed at any step.

If new water should make a contribution to the polymerization process by reacting onto intimately mixed C_3S and CSH, a larger amount of Q^2 would be detected, due to the reaction of the newly formed monomers and dimers with the preformed species.

Since this was not the case, this was a strong indication that extensive phases of C_3S react with new water by a diffusion-dominated process.

Acknowledgements

We are indebted to L. Cassar, Italcementi S.p.a., for promoting this research and to P. Persico for the preparation of the samples. This work was partly supported by CNR and MURST.

References

1. E. LIPPMAA, M. MAGI, M. TARMAK, W. WIEKER and A. R. GRIMMER, *Cement Concr. Res.* **12** (1982) 597.
2. J. HJORTH, J. SKIBSTED and J. JAKOBSEN, *ibid.* **18** (1988) 789.
3. S. A. RODGER, G. W. GROVES, N. J. CLAYDEN and C. M. DOBSON, *J. Amer. Cer. Soc.* **71** (1988) 91.
4. J. F. YOUNG, *ibid.* **71** (1988) C-118.
5. G. W. GROVES, A. BROUGH, I. G. RICHARDSON and C. M. DOBSON, *ibid.* **74** (1991) 2891.
6. R. R. ERNST, G. BODENHAUSEN and A. WOKAUN, in "Principles of nuclear magnetic resonance in one and two dimensions" (Clarendon Press, Oxford, 1991).
7. U. COSTA, *Il cemento* **76** (1979) 75.
8. D. A. TORCHIA, *J. Mag. Resonance* **30** (1978) 613.
9. E. LIPPMAA, M. MAGI, A. SAMOSON, G. ENGELHARDT and A. R. GRIMMER, *J. Amer. Chem. Soc.* **102** (1980) 4889.
10. H. F. W. TAYLOR in "Cement chemistry" (Academic Press, London, 1990).
11. N. I. GOLOVASTIKOV, R. G. MATVEEVA and N. V. BELOV, *Sov. Phys. Crystallogr.* **20** (1975) 441.
12. A. R. GRIMMER and R. RADEGLIA, *Chem. Phys. Lett.* **106** (1984) 262.
13. J. SKIBSTED, J. HJORTH and H. J. JAKOBSEN, *ibid.* **172** (1990) 279.
14. A. COMOTTI, G. CASTALDI, C. GILIOLI, G. TORRI and P. SOZZANI, unpublished.
15. A. ABRAGAM in "Principles of nuclear magnetism" (Clarendon Press, Oxford, 1989).
16. S. A. RODGER, G. W. GROVES, N. J. CLAYDEN and C. M. DOBSON, in "Microstructural Development During Hydration of Cement", in *Materials Research Society Symposia Proceedings*, Vol. 85, edited by L. J. Struble and P. W. Brown (Materials Research Society, Pittsburg, 1987) p. 13.
17. T. C. KING, C. M. DOBSON and S. A. RODGER, *J. Mater. Sci. Lett.* **7** (1988) 861.

Received 1 March
and accepted 3 June 1994